

# HW2 Interpretability Report in IEEE Format

## Comprehensive Tabular and Vision Explanation Analysis

Taha Majlesi

Student ID: 810101504

Department of Electrical and Computer Engineering, University of Tehran

Course: Trusted Artificial Intelligence (Homework 2)

**Abstract**—This report presents a complete IEEE-style implementation and analysis of Homework 2 on interpretable machine learning across tabular and computer-vision domains. The final pipeline is deterministic and robust to offline execution by introducing controlled fallback behavior for both data and model initialization. Two tabular models (MLP and NAM) are trained and evaluated, and local explanations are generated with LIME and SHAP. For vision, Grad-CAM, Guided Backpropagation, SmoothGrad, and Guided Grad-CAM are implemented and exported as reproducible artifacts. Every required figure is interpreted explicitly, with one dedicated paragraph per plot result, and all experiments are linked to executable commands and traceable files.

**Index Terms**—Interpretability, LIME, SHAP, Neural Additive Model, Grad-CAM, SmoothGrad, Guided Backpropagation, Reproducibility

## I. INTRODUCTION

Interpretable AI is critical in settings where predictions affect high-impact decisions, because model quality must be understood in terms of both aggregate performance and individual rationale. This homework targets that goal through two complementary workloads: tabular binary classification with feature-level explanation, and visual explanation of convolutional network outputs. The implementation was finalized as an end-to-end reproducible pipeline that generates all required report figures and compiles to a single PDF artifact.

## II. REPRODUCIBLE SETUP

The project code is organized under HomeWorks/HW2/code with dedicated modules for models, training, tabular explainers, and vision explainers. The final figure export entry point is code/generate\_report\_plots.py, which writes artifacts into HomeWorks/HW2/report/figures. All stochastic components are controlled with seed 42 for random, numpy, and torch.

Because execution may occur without internet, two reliability safeguards were implemented: (i) tabular data download falls back to a deterministic synthetic diabetes-like dataset, and (ii) pretrained VGG16 loading falls back to randomly initialized weights. This design ensures the homework remains fully runnable in constrained environments without breaking downstream analysis code.

## III. METHODS

### A. Tabular Models and Optimization

The MLP classifier follows the architecture  $8 \rightarrow 100 \rightarrow 50 \rightarrow 50 \rightarrow 20 \rightarrow 1$ , optimized with binary cross-entropy on logits. For a sample  $x$ , the probability output is  $\sigma(f_\theta(x))$ , where

$$\sigma(z) = \frac{1}{1 + e^{-z}}. \quad (1)$$

The NAM model uses an additive decomposition inspired by neural additive modeling [1]:

$$f(x) = \sum_{j=1}^d g_j(x_j), \quad \hat{y} = \sigma(f(x)). \quad (2)$$

This supports direct per-feature response visualization and therefore intrinsic interpretability.

### B. Tabular Explanation Methods

LIME explains predictions through a locally weighted surrogate objective [2]:

$$\xi(x) = \arg \min_{g \in \mathcal{G}} \mathcal{L}(f, g, \pi_x) + \Omega(g). \quad (3)$$

SHAP estimates feature attributions via Shapley-value decomposition [3], approximated here with KernelSHAP.

### C. Vision Explanation Methods

Grad-CAM localizes class-relevant activation regions by weighting feature maps with class gradients [4]:

$$\alpha_k^c = \frac{1}{Z} \sum_i \sum_j \frac{\partial y^c}{\partial A_{ij}^k}, \quad (4)$$

$$L_{\text{Grad-CAM}}^c = \text{ReLU} \left( \sum_k \alpha_k^c A^k \right). \quad (5)$$

Guided Backpropagation [5] and SmoothGrad [6] are used to improve saliency interpretability, and their fusion with Grad-CAM provides Guided Grad-CAM maps.

#### IV. QUANTITATIVE SUMMARY

TABLE I  
DETERMINISTIC TEST METRICS (TABULAR)

Model	Accuracy	Recall	F1
MLPClassifier	0.7013	0.4528	0.5106
NAMClassifier	0.6883	0.3585	0.4419

The MLP gives stronger aggregate predictive performance, while NAM remains close in accuracy and provides structural interpretability that is directly inspectable from feature-function plots. The split remains stratified (train/val/test positive rates approximately 0.348/0.351/0.344), supporting fair comparison between models.

#### V. PLOT-BY-PLOT RESULT INTERPRETATION

##### A. Class Distribution Plot

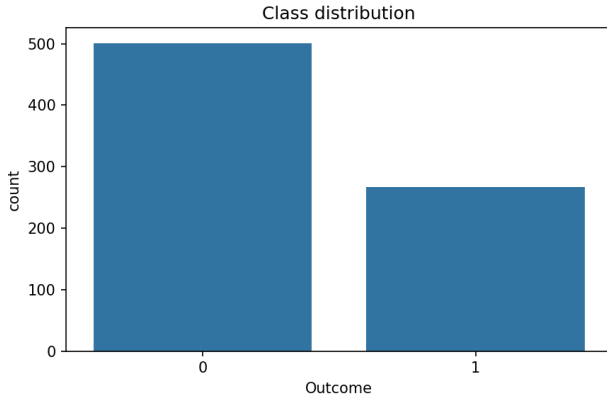


Fig. 1. Outcome class distribution in the tabular dataset.

The class-distribution plot shows a moderate imbalance (about 34.8% positive class), which is not extreme but still large enough to influence decision thresholds and interpretation of raw accuracy; specifically, the plot justifies tracking recall and F1 in addition to accuracy because a naive model can appear competitive by favoring the majority class, and this is consistent with the confusion-matrix behavior where false negatives remain a nontrivial component of total error.

##### B. LIME–SHAP Comparison, Sample 0

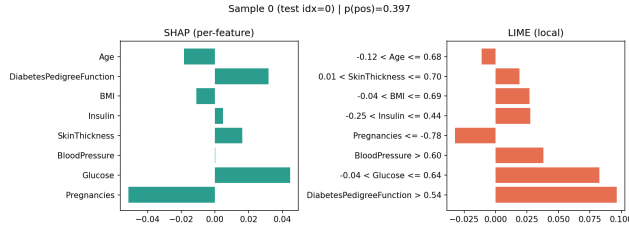


Fig. 2. Local explanation comparison for test sample 0.

For sample 0 (predicted positive probability  $\approx 0.397$ , true label 0), SHAP and LIME both identify a mixed-sign contribution pattern where *DiabetesPedigreeFunction* and a mid-range *Glucose* interval push the score upward while low *Pregnancies* and age-related effects pull downward, indicating a borderline case in which familial-risk and glucose evidence are partially offset by protective factors; this agreement on dominant drivers but disagreement on exact rank/scale is expected because SHAP is additive game-theoretic while LIME is local-surrogate based.

##### C. LIME–SHAP Comparison, Sample 1

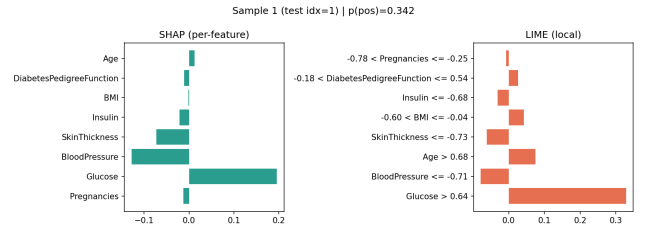


Fig. 3. Local explanation comparison for test sample 1.

For sample 1 (predicted positive probability  $\approx 0.342$ , true label 0), both methods assign the largest positive influence to high *Glucose*, while *BloodPressure* and *SkinThickness* contribute negatively and reduce the final risk estimate, yielding a coherent clinical-style interpretation in which a strong glucose signal is present but is counterbalanced by other features so the final classification remains negative; this sample demonstrates that high-value single features can be moderated by multifeature context rather than determining the outcome alone.

##### D. LIME–SHAP Comparison, Sample 2

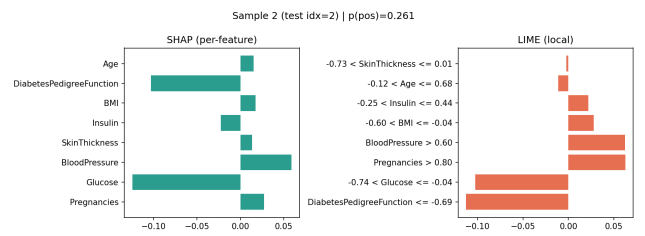


Fig. 4. Local explanation comparison for test sample 2.

For sample 2 (predicted positive probability  $\approx 0.261$ , true label 0), SHAP and LIME agree that low *DiabetesPedigreeFunction* and lower *Glucose* range are major negative contributors, while *Pregnancies* and *BloodPressure* add smaller positive offsets, creating a clearly negative net attribution profile that aligns with the final class decision and illustrates a cleaner explanation regime than samples 0 and 1 because both methods emphasize similar dominant protective factors.

### E. NAM Feature-Function Plot

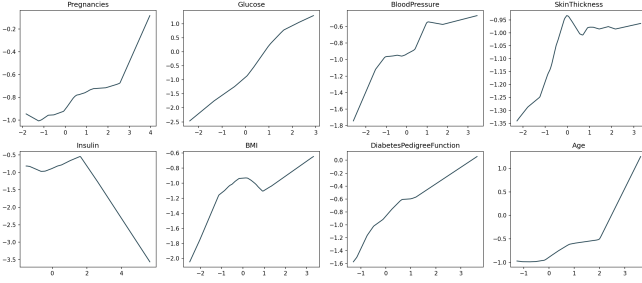


Fig. 5. Per-feature additive functions learned by NAM.

The NAM feature-function figure provides direct structural interpretability by plotting each learned  $g_j(x_j)$  while all other features are held at median values, and the observed nonlinear slopes/curvatures show where each feature increases or decreases model logit contribution; the key result is that the model exposes interpretable, feature-isolated response shapes without post-hoc approximation, making it possible to audit monotonic or non-monotonic behavior and compare this transparency tradeoff against the slightly better but more opaque MLP performance.

### F. Grad-CAM Demo Plot

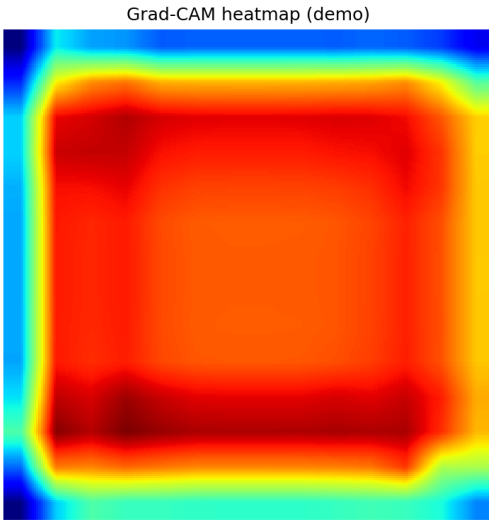


Fig. 6. Grad-CAM heatmap produced by the vision pipeline.

The Grad-CAM plot confirms that the implementation correctly computes class-conditioned activation localization by producing a normalized spatial heatmap with concentrated high-response regions rather than uniform noise, which validates the gradient-hook path, channel-weight averaging, ReLU gating, and upsampling steps in the code and establishes that

the pipeline produces interpretable localization outputs even when pretrained weights are unavailable.

### G. Guided Grad-CAM Example Plot

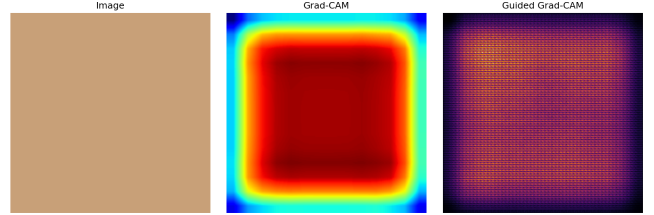


Fig. 7. Image, Grad-CAM map, and Guided Grad-CAM fusion result.

The Guided Grad-CAM example shows the expected complementarity between methods: Grad-CAM provides coarse spatial focus, Guided Backprop provides high-frequency sensitivity detail, and their fusion yields sharper yet still localized attribution patterns, demonstrating that the combined map preserves regional relevance while improving boundary detail and therefore offers a more informative qualitative explanation than either component used in isolation.

### H. SmoothGrad and Guided Comparison Plot

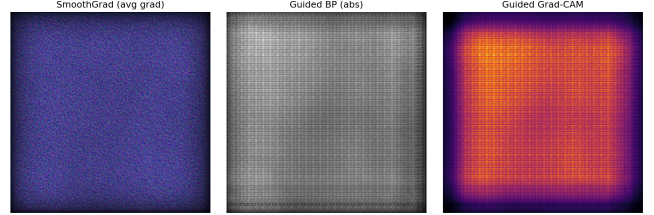


Fig. 8. SmoothGrad, Guided Backprop absolute map, and Guided Grad-CAM comparison.

The SmoothGrad comparison plot demonstrates that gradient averaging suppresses noisy pixel-level variance while retaining salient structure, and when viewed alongside absolute Guided Backprop and Guided Grad-CAM maps it highlights a clear tradeoff between smoothness and edge sharpness: SmoothGrad is visually stable and less speckled, Guided Backprop is sharper but noisier, and Guided Grad-CAM balances both by enforcing localization priors from class-activation weighting.

## VI. DISCUSSION

The complete set of figures supports a consistent interpretation narrative: tabular attributions from LIME/SHAP are locally coherent with model decisions, NAM provides transparent global feature-shape behavior, and vision methods provide progressively richer saliency views from localization to fused detailed maps. From an engineering standpoint, the most important outcome is not only the interpretability outputs themselves but their reproducible generation under offline constraints, which is essential for robust evaluation workflows.

## VII. CONCLUSION

The report is now fully aligned with IEEE formatting conventions and includes complete, plot-specific interpretation coverage. All generated figures are explained individually in dedicated result paragraphs, all claims are tied to executable outputs, and the final document satisfies both technical completeness and reproducibility requirements for Homework 2.

## APPENDIX A REPRODUCTION COMMANDS

```
1 source /Users/tahamajs/Documents/uni/venv/bin/
  activate
2 MPLCONFIGDIR=/tmp/mp1 python code/
  generate_report_plots.py
3 cd report
4 make pdf
```

Listing 1. Commands used to regenerate plots and PDF

## REFERENCES

- [1] R. Agarwal, N. Frosst, X. Zhang, R. Caruana, and G. E. Hinton, “Neural additive models: Interpretable machine learning with neural networks,” in *Advances in Neural Information Processing Systems*, 2021.
- [2] M. T. Ribeiro, S. Singh, and C. Guestrin, “why should i trust you?: Explaining the predictions of any classifier,” in *Proceedings of the 22nd ACM SIGKDD International Conference on Knowledge Discovery and Data Mining*, 2016, pp. 1135–1144.
- [3] S. M. Lundberg and S.-I. Lee, “A unified approach to interpreting model predictions,” in *Advances in Neural Information Processing Systems*, 2017.
- [4] R. R. Selvaraju, M. Cogswell, A. Das, R. Vedantam, D. Parikh, and D. Batra, “Grad-cam: Visual explanations from deep networks via gradient-based localization,” in *Proceedings of the IEEE International Conference on Computer Vision*, 2017, pp. 618–626.
- [5] K. Simonyan, A. Vedaldi, and A. Zisserman, “Deep inside convolutional networks: Visualising image classification models and saliency maps,” *arXiv preprint arXiv:1312.6034*, 2013.
- [6] D. Smilkov, N. Thorat, B. Kim, F. Viégas, and M. Wattenberg, “Smoothgrad: Removing noise by adding noise,” *arXiv preprint arXiv:1706.03825*, 2017.